DETECTION OF He II λ4686 IN η CARINAE[1]

J. E. Steiner and A. Damineli

Instituto de Astronomia, Geofísica e Ciências Atmosféricas, University of São Paulo, Rua do Matão 1226, 05508-900 São Paulo, Brazil;
steiner@astro.iag.usp.br, damineli@astro.iag.usp.br

ABSTRACT

We report the detection of the emission line He II λ4686 in η Carinae. The equivalent width of this line is ~100 mÅ along most of the 5.5 yr cycle and jumps to ~900 mÅ just before phase 1.0, followed by a brief disappearance. The similarity between the intensity variations of this line and those of the X-ray light curve is remarkable, suggesting that they are physically connected. We show that the expected number of ionizing photons in the ultraviolet and soft X-rays, expected to be emitted in the shock front from the colliding winds, is of the order of magnitude required to produce the He II emission via photoionization. The emission is clearly blueshifted when the line is strong. The radial velocity of the line is generally -100 km s^{-1}, decreases steadily just before the event, and reaches -400 km s^{-1} at phase 1.001. At this point, the velocity gradient suddenly changes sign, at the same time that the emission intensity drops to nearly zero. Possible scenarios for explaining this emission are briefly discussed. The timing of the peak of He II intensity is likely to be associated with the periastron and may be a reliable fiducial mark, important for constraining the orbital parameters.

Subject headings: binaries: general — stars: early-type — stars: individual (η Carinae)

1. INTRODUCTION

Massive stars have a strong impact on galactic environments. Their evolution, however, is not very well known because their intrinsic parameters are difficult to determine. This is even more true for the mass, which requires a binary companion to be weighted. The luminous blue variable η Carinae, believed to be one of the most massive stars known from its luminosity, has shown signatures of binarity, opening up the possibility of measuring this fundamental parameter.

The first evidence of binarity emerged from the true periodicity in the 5.5 yr cycle (Damineli 1996; van Genderen et al. 2003; Whitelock et al. 2004; M. F. Corcoran et al. 2004, in preparation). The second step to unveiling the binary nature of the star was done when specific models could be calculated. Damineli et al. (1997, hereafter DCL) derived highly eccentric orbits from radial velocities of Paschen lines and suggested that X-rays are produced by wind-wind collision. That particular model had problems because emission lines do not trace the orbital motion precisely (Davidson 1997). However, parameters similar to that of DCL were used to reproduce the main features of the X-ray emission in η Car by wind-wind collision models (Corcoran et al. 2001; Pittard & Corcoran 2002, hereafter PC). The orbital parameters, however, are still not well constrained.

The subject of this Letter is to present the unexpected detection of the He II λ4686 variable emission line in η Car and to explore how it is related to the binary nature of the star.

2. OBSERVATIONS AND RESULTS

The data presented here are part of a long-term spectroscopic monitoring of η Car, started in 1989 at the coudé focus of the 1.6 m telescope of the Pico dos Dias Observatory (LNA/Brazil). Full results, including the analysis of many low- and high-excitation lines, will be reported in A. Damineli et al. (2004, in preparation), from which we are using the period length $P = 2022.1$ days (5.536 yr) and the time of phase zero (phase 0.0) of the spectroscopic event (JD = 2,452,819.8, 2003

June 29), defined by the disappearance of the narrow component in the He I λ6678 line.

Data reduction was done with the IRAF package in the standard way. The spectral resolution was degraded to 0.5 Å pixel^{-1} in order to enhance the signal-to-noise ratio (S/N). Most of the spectra used here have S/N > 100 in the stellar continuum, and some of them twice as much, specially around phases 0.2–0.8, when many spectra were co-added. We detected an emission line at ~4680–4685 Å (Fig. 1), which we suggest to be He II λ4686. We searched for possible transitions in the range 4670–4700 Å and found none from species that are typical of the η Carinae spectrum. He II λ4686 has never been detected with certainty before, as discussed by Hillier & Allen (1992 and references therein), who reported an upper limit of 1 Å. The line showed up in almost all of our high-quality spectra, except in a few of lower S/N. Paradoxically, this line is faint in high-excitation phases and strong during the event, contrary to the behavior of the high-excitation forbidden lines. In Figure 1 we display a sample of spectra collected in 2003, ordered by phase of the 2022.1 day period.

In order to evaluate the errors, we measured each line several times, with different assumptions for the continuum. The errors were 20–100 mÅ in the equivalent widths (EWs) and 10–110 km s^{-1} in the radial velocities (RVs) of the line centroid (V_{cen}) and are displayed in Figures 2 and 3. Those are formal errors; systematic errors may also be present, for example, if introduced by the rectification of the continuum. The fit to the continuum was done by a third-order polynomial, which introduces only low frequencies and has little influence on scales comparable to the extent of a spectral line. Structures in the flat-fielding image could introduce distortions in the continuum, although of low frequency, since we always used the same observational setup and data reduction procedures. The EWs are affected by an additional type of systematic error, line blending, which prevents the assessment of the local continuum and consequently the extension of the line wings. This makes the measurements of EWs and the FWHM (~500–600 km s^{-1}) somewhat underestimated, as is the case for almost all other spectral lines in the rich spectrum of η Car. The position of
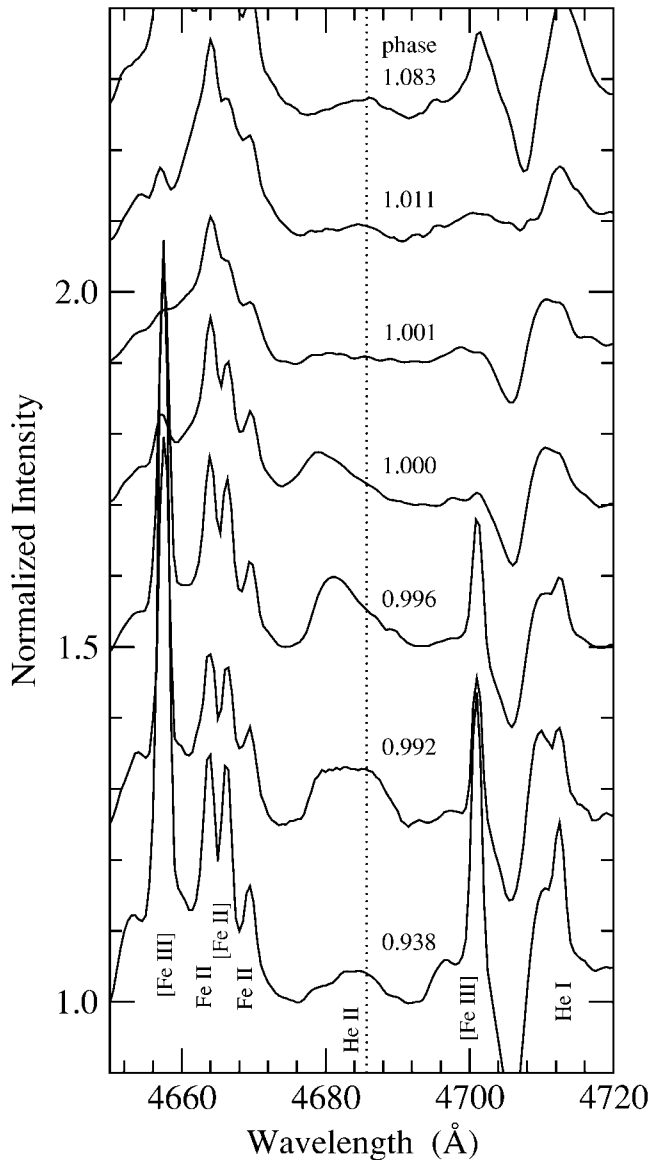
Fig. 1.—Sample of He II λ4686 line profiles labeled by phase of the 2022.1 day period. The vertical dotted line indicates the rest wavelength of He II λ4686.

the line centroid is much more robust and is affected only by the S/N; consequently the errors can be better judged from the overall scatter in the RV curve.

The slit width was kept fixed at ~1″5, and this seems relevant, since a fraction of the He II emission appears to be extended. Our data of 1997 and 2002, when compared with contemporaneous spectra taken with the Fiber-fed Extended Range Optical Spectrograph at ESO (~3″6 fiber entrance), result in smaller EWs. The comparison of our 2003 data with those taken with the Space Telescope Imaging Spectrograph (STIS) on board of the *Hubble Space Telescope* (*HST*; ≈0″1 slit width) results in larger EWs, indicating that the EWs are larger for wider slits. This is the opposite of that reported by Hillier & Allen (1992) for H I, He I, and Fe II lines in the Homunculus, which are smaller than those in the central object. He II seems to be intrinsically in emission near the central source since dust scattering would preserve the equivalent widths. The line shape and radial velocity are unchanged with the slit aperture, indicating that most of the emission should arise from the central
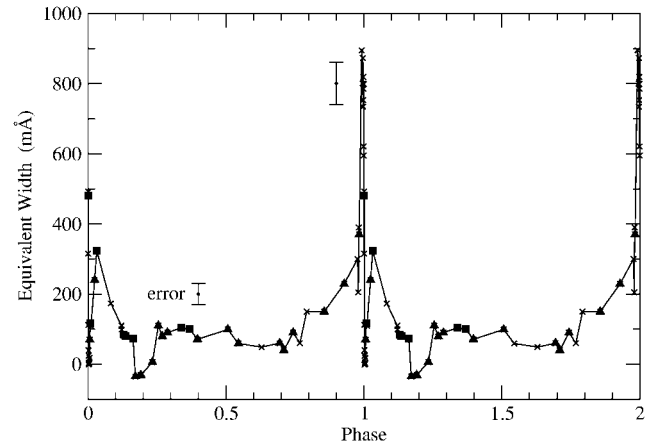

Fig. 2.—He II λ4686 line EW curve for the last three cycles: The filled triangles are for 1997/98; the filled squares for 1992; and the crosses are for 2003.

object. In fact, long-slit CCD *HST*/STIS spectra (52″ × 0″1) collected prior to the 2003.5 event (T. R. Gull 2004, private communication) show that the He II emission was confined to 0″1 (2 pixel limit) in the east-west direction. However, the emission could be extended in other directions outside the slit. Although this question is relevant, the data available to us are insufficient to derive any firm conclusion, and therefore we will restrict our analysis to the homogeneous Brazilian set of data.

In Figure 2 we see that the strength of the He II line is very weak along the 5.5 yr cycle at the level of EW ≈ 100 mÅ. It starts strengthening around phase ≈0.8, jumps to EW = 873 mÅ just before phase 1.0, and after a brief fading
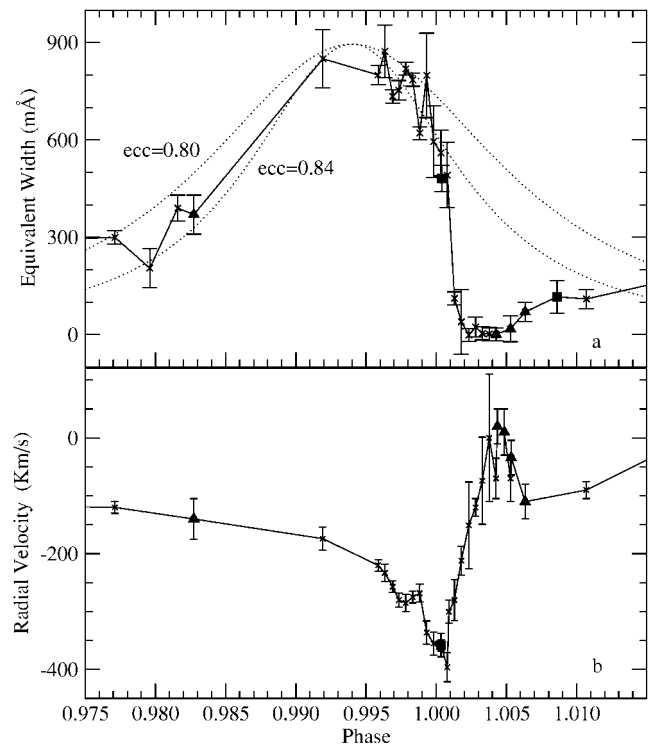

Fig. 3.—Zoom-in He II λ4686 variations around phase 0. In panel *a*, the solid line represents the EW curve, and the dotted lines represent He II emission models. In panel *b*, we present the RV curve, which has the same symbols as in Fig. 2.

it rises again, reaching a local maximum (EW = 300 mÅ) at phase ≈1.04. In Figure 3a we display a zoom-in the EW curve around phase 1.0, showing a peak centered at phase 0.994, a fast drop after phase 1.0, and a minimum around phase 1.003. In Figure 3b we show the RV curve as measured from the velocity of the line centroid. The velocity becomes more and more negative as the system approaches phase 1.0, reaching a sharp minimum ($V_{cen} = -396$ km s^{-1}) at phase 1.001. After phase 1.002, uncertainties in RVs increase significantly, and therefore we will not comment them any further.

3. INTERPRETATION AND DISCUSSION

The interpretation of the intensity curve of He II λ4686 as well as of its radial velocity may provide important insights about the nature and structure of the system. The first thing to notice is the strong similarity between the He II emission curve and the X-ray light curve (Corcoran et al. 2001; Ishibashi et al. 1999). Both emissions start to enhance at phase 0.8, peak just before phase 1.0, drop to near zero intensity at about phase 1.001, and return to normal intensity after phase ~1.1. A noticeable difference between the two light curves is that He II has a much narrower and prominent peak (centered at phase 0.994) than the X-ray light curve, which has its maximum at phase 0.985. The X-ray emission is thought to originate from the shock front of the colliding winds in a binary system. Its "eclipse" has been modeled by PC, who derived system parameters that will be adopted as a reference frame in the following discussion. Given this similarity, it is tempting to interpret the He II emission as originating from photoionization by X-ray or ultraviolet (UV) photons associated with this source.

Near periastron, the X-ray and UV ionizing photons are mostly unobserved as they are absorbed by the intervening gas along the line of sight. However, gas near the shock front (including the winds of the primary and secondary stars) may still be directly exposed to this ionization. He II λ4686, at its maximum intensity, has a luminosity of $L_{\mathrm{He\,II}} \sim 100\ L_\odot$ (assuming the somewhat uncertain values of $V \sim 7.5$ and $A_V \sim 6$ for the central source). This amounts to about 9×10^{46} photons s^{-1}. In order to produce this emission, a luminous source of ionizing soft X-ray and UV photons is required; the peak luminosity of the unabsorbed X-rays in the range 2–10 keV is only $L_{\mathrm{Xunabs}} = 67\ L_\odot$ (Ishibashi et al. 1999). Detailed hydrodynamical numerical calculations by PC show that when the velocity of the secondary's wind is large ($V_2 \sim 3000$ km s^{-1}), the energy spectrum behaves like a power law, at soft X-rays. From their Figure 3 we derive a spectrum of $L_\epsilon = 2.5 \times 10^{35}\epsilon^{-2.7}$ ergs s^{-1} keV^{-1} for the system parameters favored by those authors ($\dot{M}_2 = 10^{-5}\ M_\odot$ yr^{-1} and $V_2 = 3000$ km s^{-1}). In the case where this spectrum can be extrapolated down to 54 eV (He$^+$ threshold ionization), the total luminosity would be $L_{\mathrm{ion}} = 5200\ L_\odot$. This extrapolation seems to be reasonable since the energy loss by the wind from the secondary star alone is $\dot{E}_2 = 7500\ L_\odot$. The total number of photons emitted by this source is $\dot{N}_{\mathrm{ion}} = 2.5 \times 10^{47}$ photons s^{-1}, which amounts to ≈3 times the observed number of He II λ4686 photons. If we add to this the energy from the shock of the primary star, this number will be even larger. We conclude that near periastron, the production of ionizing photons is of the right order of magnitude to produce the observed He II emission via photoioniozation. It is worth noting that only ≈1% of the kinetic energy from the wind of the secondary star is radiated in the 2–10 keV band. Where are the other 99% going to? The detection of He II emission may be the first hint that they are mostly radiated in the UV.

The fact that the bulk of the He II emission is short-lived in terms of the EW curve (lasting for ≈1% of the orbital cycle) suggests that its peak indicates the passage of the periastron, and this is quite interesting. This timing is not precisely determined either by the X-ray light curve (as the wind of the primary star is optically thick to X-ray absorption) or by the high-excitation emission lines (which are emitted far away), although the low-ionization event is generally believed to be associated with the periastron approach. The timing of the periastron (phase 0.994) would be the second orbital parameter determined with accuracy, besides the period.

A solution to the X-ray light curve was obtained by PC in which the wind-wind shock before eclipse is observed through the opening angle in such a way that the X-ray source is seen through the nonabsorbing wind from the secondary star. After the shock front passes through the line of sight, the X-rays are absorbed by the wind from the primary star. In this way the symmetry of the observed emission is broken, and one gets a postminimum flux that is lower then the preminimum one. If we assume that the periastron passage occurs at phase 0.994, we are able to fit the X-ray light curve with the following parameters: eccentricity $e = 0.84$ and the longitude of the periastron of the primary star, $\omega = 212°$. These parameters predict a superior conjunction for the secondary star with a true anomaly of $\theta = 58°$ at the phase where our observations show a sharp drop in EWs and a gradient reversal in the RV curve. Does this suggest an eclipse? This question brings us to another one: where is the region of He II emission located?

The large values of the velocity cannot be associated with the shock front itself since the gas in that region has nearly the velocity of the center of mass. A similar argument could be made with respect to the wind of the primary star. The terminal velocity of the primary star is about ~500 km s^{-1}; at the phase under consideration, the shock front is quite near the primary, and the velocity of the wind is still far from terminal. In addition, the shock front is symmetric with respect to the orbital plane, and the line of sight imposes a projection of $i \sim 45°$. In this scenario, it seems difficult to combine the emission and radial velocity behavior as displayed in Figure 3. In particular, the radial velocity is bluest when the emission has dropped to its half-maximum intensity, after reaching the peak. If we suppose that the emission comes from the near side of the primary star, ionized to He^{++} by the secondary or by the shock, one would expect maximum blueshift at maximum emission.

Perhaps a more promising explanation is that the He II emission comes from the wind of the secondary star, ionized by the external UV emission from the shock front. This would produce an ionization front that divides this wind into a zone of He$^+$ and a zone of He^{++}. The He^{++} zone would be directly exposed to the UV emission, and an asymmetric configuration would be produced with respect to the secondary star. This asymmetry will cause a blueshifted emission when the system is seen at an appropriate angle. As periastron occurs at phase 0.994 and the longitude of periastron is $\omega = 212°$, the ionized He II–emitting wind from the secondary star should naturally display negative velocities when seen from the line of sight of the observer. The terminal velocity of the wind from the secondary star is about ~3000 km s^{-1} (PC), so one might expect higher velocities and line widths than observed. However, the emission is likely to come from deep in the wind where the density is higher and the velocity smaller, still far from the terminal velocity. In addition, the inclination of the system is about $i \approx 45°$, which reduces the velocity by about ~cos i. Let us assume a highly idealized model of an ionized hemisphere

with concentric layers of radii r and a normal velocity law: $v = v_0(1 - R_2/r)^\beta$ (where R_2 is the radius of the secondary star). As the emissivity is proportional to the square of the density, the contribution of each layer to the line intensity is proportional to $\sim r^{-2}$. The peak of the line profile should, therefore, be emitted at velocities that correspond to the innermost ionized zone. We estimate that in order to produce the observed RVs (-400 km s^{-1}), the innermost ionized zone should occur at $r \approx 4R_2$, for $\beta = 1$. At periastron, the distance from the secondary star to the innermost zone is 60 $R_\odot$, the distance from the secondary star to the stagnation shock front is 210 $R_\odot$, and the distance from the secondary star to the surface of the primary is 360 $R_\odot$.

The observed line widths (FWHM $\sim$ 500–600 km s^{-1}) require a radius that is somewhat smaller. However, as pointed out before, the observed FWHM is a lower limit because the line wings/continuum are difficult to determine with accuracy. If the He II–emitting wind is indeed eclipsed, one would expect that when the intensity is at its half-maximum, half of the wind should be eclipsed, and the velocity should be most negative; this is so because, given the structure of the shock front and its skew angle (see PC), at this time the portion of the wind with more positive velocity is already eclipsed. This prediction is confirmed as both events occur at the same phase (phase 1.001).

The sharpness of the fading phase of the He II intensity curve (Fig. 3a) is a challenging characteristic that demands restrictive parameters to be modeled. For example, if it is due to an eclipse that would be caused by the primary star or by its wind, this wind cannot be isotropic with a mass-loss rate of $\dot{M}_1 = 2.5 \times 10^{-4}$ $M_\odot$ yr^{-1} (PC); this would be optically thick for electron scattering at too large a radius. As an alternative, one could suppose that the Homunculus configuration, with a bipolar and equatorial disk, could be scaled down to the size of the binary system. In this situation, the polar wind would be

responsible (partially if not totally) for the eclipse of the He II emission and the equatorial disk and for the X-ray–emitting shock front. Such a configuration has also been proposed on the basis of other observational (Smith et al. 2003; van Boekel et al. 2003) and theoretical (Maeder & Desjacques 2001) considerations. However, results from spectral modeling in the optical (Hillier et al. 2001) and infrared interferometry (van Boekel et al. 2003) have found mass-loss rates of $\dot{M}_1 \sim 10^{-3}$ $M_\odot$ yr^{-1}. Such determinations are clearly in contradiction with our eclipse hypothesis, unless the mass-loss rate is highly anisotropic.

In the wind-wind collision model, the X-ray luminosity is inversely proportional to the separation of the stars, $L_X \alpha D^{-1}$, so that at periastron, X-ray luminosity is maximum (Usov 1992). At the same time, the angle subtended by the secondary star as seen from each point of the shock front is αD^{-1}, making the fraction of the UV and X-ray photons that is absorbed by the wind from the secondary star go with the square of the inverse of the distance between the two stars. Therefore, one expects the luminosity of the He II line to be inversely proportional to the cube of the stellar separation: $L_{\text{He II}} \alpha D^{-3}$. Figure 3 shows that the rising phase and the peak of the He II EW curve can be well described by a function of the form $L_{\text{He II}} \alpha D^{-3}$ for $e = 0.82$–0.84. This agreement, however, does not prove that the He II emission comes from the wind of the secondary star; any model that provides a dependence as the inverse of the cube of the distance would be just as good.

In this simplified model we suppose that the emission is highly concentrated. We should keep in mind that there are indications for extended emission as well, so that the real picture is actually more complicated, but its detailed analysis and modeling are beyond the scope of this Letter.

REFERENCES

Corcoran, M. F., Ishibashi, K., Swank, J. H., & Petre, R. 2001, ApJ, 547, 1034
Damineli, A. 1996, ApJ, 460, L49
Damineli, A., Conti, P. S., & Lopes, D. F. 1997, NewA, 2, 107 (DCL)
Davidson, K. 1997, NewA, 2, 387
Hillier, D. J., Davidson, K., Ishibashi, K., & Gull, T. 2001, ApJ, 553, 837
Hillier, J. D., & Allen, D. A. 1992, A&A, 262, 153
Ishibashi, K., Corcoran, M. F., Davidson, K., Swank, J. H., Petre, R., Drake, S. A., Damineli, A., & White, S. 1999, ApJ, 524, 983

Maeder, A., & Desjacques, V. 2001, A&A, 372, L9
Pittard, J. M., & Corcoran, M. F. 2002, A&A, 383, 636 (PC)
Smith, N., Gull, T. R., Ishibashi, K., & Hillier, J. 2003, ApJ, 586, 432
Usov, V. V. 1992, ApJ, 389, 635
van Boekel, R., et al. 2003, A&A, 410, L37
van Genderen, A., Sterken, C., Allen, W. H., & Liller, W. 2003, A&A, 412, L25
Whitelock, P., Feast, M. W., Marang, F., & Breedt, E. 2004, MNRAS, 352, 447